# Polyploid cancer cells reveal signatures of chemotherapy resistance

Michael J. Schmidt[1], Amin Naghdloo[1], Rishvanth K. Prabakar[1,2], Mohamed Kamal[1,3], Radu Cadaneanu[4], Isla P. Garraway[4], Michael Lewis[5-7], Ana Aparicio[8], Amado Zurita-Saavedra[8], Paul Corn[8], Peter Kuhn[1], Kenneth J. Pienta[9], Sarah R. Amend[9*], James Hicks[1*]

1. Convergent Science Institute in Cancer, Michelson Center for Convergent Bioscience, University of Southern California, Los Angeles, California, USA.
2. Currently at: Simons Center for Quantitative Biology, Cold Spring Harbor Laboratory, Cold Spring Harbor, NY, USA.
3. Department of Zoology, Faculty of Science, Benha University, Benha, Egypt.
4. Department of Urology, Jonsson Comprehensive Cancer Center, David Geffen School of Medicine at UCLA and VA Greater Los Angeles, University of California, Los Angeles, Los Angeles, California, USA.
5. VA Greater Los Angeles Medical Center, Los Angeles, CA, USA.
6. Departments of Medicine and Pathology, Cedars-Sinai Medical Center, Los Angeles, CA, USA.
7. Center for Cancer Research and Cellular Therapeutics, Clark, Atlanta, GA, USA.
8. Department of Genitourinary Medical Oncology, The University of Texas MD Anderson Cancer Center, Houston, TX, USA.
9. Cancer Ecology Center, The Brady Urological Institute, Johns Hopkins University School of Medicine, Baltimore, MD, USA.

*Corresponding Authors: samend2@jhmi.edu; jameshic@usc.edu

## Abstract

Therapeutic resistance in cancer significantly contributes to mortality, with many patients eventually experiencing recurrence after initial treatment responses. Recent studies have identified therapy-resistant large polyploid cancer cells in patient tissues, particularly in late-stage prostate cancer, linking them to advanced disease and relapse. Here, we analyzed bone marrow aspirates from 44 advanced prostate cancer patients and found the presence of circulating tumor cells with increased genomic content (CTC-IGC) was significantly associated with poorer progression-free survival. Single cell copy number profiling of CTC-IGC displayed clonal origins with typical CTCs, suggesting complete polyploidization. Induced polyploid cancer cells from PC3 and MDA-MB-231 cell lines treated with docetaxel or cisplatin were examined through single cell DNA sequencing, RNA sequencing, and protein immunofluorescence. Novel RNA and protein markers, including HOMER1, TNFRSF9, and LRP1, were identified as linked to chemotherapy resistance. These markers were also present in a subset of patient CTCs and associated with recurrence in public gene expression data. This study highlights the prognostic significance of large polyploid tumor cells, their role in chemotherapy resistance, and their expression of markers tied to cancer relapse, offering new potential avenues for therapeutic development.

70

## Keywords

polyploid giant cancer cell; circulating tumor cell; progression-free survival; liquid biopsy; polyaneuploid cancer cell state; chemotherapy resistance; single cell

75

## 1. Introduction

While initial treatment efficacy is observed in most patients with prostate or breast cancer, prostate cancers recur in 24-48% of cases [1], and breast cancers relapse in about 30% of patients [2-3]. In general, late-stage metastatic cancers are more difficult to control, and patients are typically treated with chemotherapy; unfortunately, complete response rates from chemotherapy treatments in patients with late stage disease are low [4-5]. Despite defining numerous detailed intrinsic and extrinsic mechanisms that enable cancer cell survival under therapy, therapy resistance remains responsible for over 90% of cancer related deaths [6-8].

Large polyploid tumor cells are correlated with late disease stages, poor prognosis, and therapy resistance across virtually every tumor type [9-13]. Large polyploid tumor cells are induced through various stressors, including common chemotherapies such as docetaxel and cisplatin [14-17]. Evidence has shown that whole genome doubling (WGD) events and altered ploidy levels are poor prognostic indicators across cancer types and are

3

95  ultimately thought to provide cancer cells the ability to evolve and

96  survive therapy [18-21].

97       Recent studies have shown that large polyploid tumor cells

98  can give rise to viable progeny that display more malignant and

99  stem cell characteristics than the parental population they

100  descended from [22]. Importantly, targeting identified pathways,

101  including AP-1, HIF2a, cholesterol-related, and embryogenic-

102  related pathways, reduced the number of surviving large polyploid

103  cancer cells, as well as surviving progeny cells following therapy

104  [22-26]. While significant, these studies lack single-cell molecular

105  resolution and note that not all cells are eliminated. What

106  ultimately matters is that some cancer cells are still capable of

107  survival and result in disease progression. Identification of novel

108  biomarkers that can predict patients' recurrence and resistance to

109  therapy may lead to better treatment outcomes.

110       We find that the presence of circulating tumor cells (CTCs)

111  with increased genomic content in the bone marrow aspirate of

112  late-stage prostate cancer patients is significantly associated with

113  worse progression free survival. We comprehensively evaluated

114  large polyploid tumor cells (prostate cancer PC3 and breast

115  cancer MDA-MB-231) that survive following treatment with two

116  chemotherapy classes (cisplatin and docetaxel), and functionally

117  characterize the surviving cells through a multi-omic approach,

118  including morphometric, genomic, and transcriptomic profiling at

119  the single cell level. We find that progeny cells differed

120  substantially from the original parental population and most

4

121 closely resembled the transcriptome of the large polyploid tumor

122 cells from which they were derived. We also find novel markers

123 associated with chemotherapy survival are upregulated in cells

124 that survive treatment, are retained in the progeny from surviving

125 cells, and are significantly associated with recurrence in prostate

126 and breast cancer at the RNA level. These novel survival

127 biomarkers are expressed at the protein level in the CTCs of

128 patients who also have recurrent disease. Taken together, our

129 results highlight novel biomarkers of survival and shed light on the

130 functionality of large polyploid tumor cells and their role in disease

131 recurrence.

132

## 2. Methods

134 **Patient sample collection and processing**: Liquid biopsy

135 samples were collected from clinical sites and processed at the

136 University of Southern California as previously described [27-28].

137 Briefly, peripheral blood (PB) and bone marrow aspirate (BM)

138 samples were collected from patients immediately starting

139 treatment on trial NCT01505868 that evaluated cabazitaxel with or

140 without carboplatin in patients with metastatic castration-resistant

141 prostate cancer. Samples were collected at MD Anderson Cancer

142 Center prior to therapy.

143 Patients 1 and 3 did not participate in NCT01505868.

144 Patient 1, a previous case study, was acquired from the Greater

145 Los Angeles Veterans' Affairs Healthcare System [29]. The bone

146 marrow sample was collected at the time of diagnostic biopsy,

147 prior to treatment. Patient 3, another previous case study [30],

148 was acquired from MD Anderson. All patients gave written

149 informed consent in accordance with approved institutional review

150 board and research development (VA) protocols.

151 Following isotonic erythrocyte lysis, the entire nucleated

152 fraction was plated onto custom cell adhesion glass slides

153 (Marienfield, Lauda, Germany) and stored at -80°C until use [28].

154 **Cell culture and drug treatment**: PC3 and MDA-MB-231 cell

155 lines were purchased from ATCC and grown in RPMI and DMEM,

156 respectively, with 10% FBS and 0.5% penicillin / streptavidin. Cells

157 were plated at a density of 625,000 cells per T-75 flask. PC3 cells

158 were treated with 5 nM docetaxel (PC3: 5nM, MDA-MB-221:

159 10nM) or cisplatin (10 µM) for 72 hours. Cells were then allowed

160 to recover in normal medium for 1 or 10 days. When indicated,

161 PC3 cells were re-treated at day 10 post treatment removal. Cells

162 were lifted from culture and plated on Marienfield glass slides for

163 imaging or single cell isolation. All cell line experiments were

164 conducted in triplicate.

165 To isolate progeny cells, PC3 cells 10 days post treatment

166 were lifted with 1x versene. Biosorter (UnionBio, Holliston, MA)

167 was used to sort single cells based on size and the largest 15% of

168 cells were sorted into ten 96-well plates (n=960 individual wells)

169 containing RPMI medium and then placed in a 37°C incubator.

170 Media was changed every 2-3 days.

171 **Immunofluorescent staining:** Patient slides in Figure 1 were

172 fixed with paraformaldehyde and stained with a pan-cytokeratin

173 cocktail mixture (see supplementary methods), conjugated mouse

174 anti-human CD45 Alexa Fluor 647 (clone: F10-89-4, MCA87A647,

175 AbD Serotec, Raleigh, NC, USA), Vimentin (Alexa Fluor 488 rabbit

176 IgG monoclonal antibody (Cell Signaling Technology; Cat#

177 9854BC; Clone: D21H), and 4',6-diamidino-2-phenylindole (DAPI;

178 D1306, Thermo, Waltham, MA, USA) as previously described [28].

179 EpCAM (Thermo, 14-9326-82) was included in the pan-cytokeratin

180 cocktail mixture to make an "EPI-cocktail".

181 TNFRSF9 (Thermo, PA5-98296) and HOMER1 (Thermo,

182 PA5-21487) primary antibodies were incubated on slides overnight

183 at 4°C with the EPI-cocktail of antibodies. Slides were then

184 washed and incubated at room temperature for two hours with

185 Alexa Fluor 555 goat anti-mouse IgG1 antibody (Thermo,

186 A21127), Alexa Fluor 488 goat anti-rabbit (Thermo, A11034),

187 CD45, and DAPI.

188 LRP1 (Thermo, 377600) was generated in mice and was

189 therefore not compatible with the EPI-cocktail. Instead, LRP1 was

190 incubated overnight at 4°C. Slides were then washed and

191 incubated at room temperature for two hours with Alexa Fluor 555

192 goat anti-mouse IgG1 antibody. Next, pre-conjugated Alexa Fluor

193 488 pan-cytokeratin (53-9003-82, Thermo) recognizing CK 10, 14,

194 15, 16, and 19 was incubated with conjugated mouse anti-human

195 CD45, and DAPI.

7

196 **Slide imaging and analysis**: Slides were imaged with an

197 automated high throughput microscope equipped with a 10x

198 optical lens, as previously described [27]. Immunofluorescent and

199 bright field images were collected. Image analysis tool, available

200 at https://github.com/aminnaghdloo/slide-image-utils, was

201 developed in python using the OpenCV and scikit-image

202 packages [31-32]. Briefly, each fluorescent channel was

203 segmented individually using adaptive thresholding and merged

204 into one cell mask. Cell mask and DAPI mask were used to

205 extract features and fluorescent intensity statistics of single cells

206 and their nuclei, respectively. For nucleus size analysis, equivalent

207 diameter was calculated from nucleus area, assuming a circular

208 shape.

209 **Fluorescence *in situ* Hybridization**: Probes for centromeres of

210 chromosomes 1 (CHR01-10-GR) and 10 (CHR10-10-GR) were

211 purchased from Empire Genomics (Depew, New York) and the

212 hybridization was carried out on Marienfeld glass slides per the

213 manufacturer's instructions. Slides were then stained with DAPI

214 and then imaged.

215 **Single cell copy number profiling**: Single cells were isolated as

216 previously described [28]. Copy number profiling from low pass

217 whole genome sequencing samples was conducted as previously

218 described (see supplementary methods) [33-34].

219 **Single cell RNA sequencing**: Single cells were isolated and

220 picked via micro-manipulation as previously described. RNA was

221 extracted via a modified Smart-Seq2 approach and library

8

222    prepped with Nextera XT (Illumina, San Diego, CA). Cells were

223    sequenced paired end by 150 base-pairs on an Illumina HiSeq

224    4000 (Fulgent). Read adapters were trimmed with TrimGalore

225    (version 0.6.7) and aligned with the HiSat2 (v2.2.1). Picard

226    (v3.0.0) was used to visualize RNA mapping quality control [35-

227    37]. HTSeq (v2.0.2) was used to generate a gene count matrix

228    [38].

229    The SingleCellExperiment package (v4.2.2) was utilized for

230    inputting count data into downstream analyses, such as

231    converting to Seurat (v4.3.0) and edgeR (v3.36.0) count matrices

232    [39]. Downstream analysis was performed with R (v4.1.2). Data

233    visualization was performed with Seurat and ggplot2 (v3.4.4), and

234    Pheatmap (v1.0.12) packages.

235    The edgeRQLFDetRate differential expression pipeline

236    was used to find common upregulated genes in polyploid cancer

237    cells [40]. Sequencing batches were controlled for. Shared genes

238    expressed in surviving large cells were intersected through R.

239    Gene datasets were downloaded directly from CHEA3 [41]

240    and MSigDB [42] for transcription factor and hallmark pathway

241    enrichment, respectively. Single cell enrichment was conducted

242    through JASMINE [43].

243

244    **Survival analysis**: Survival analysis from patient bone marrow

245    and peripheral blood samples was performed with the Survival R

246    package (v3.5.5) and plotted with ggplot2 (v3.4.4). Public gene

247    expression survival analysis was analyzed via PanCancSurvPlot

248   [44] for prostate cancer (GSE116918) and breast cancer

249   (GSE10893) [45-46].

250

## 3. Results

252   **CTCs with increased genomic content (CTC-IGC) are found in**

253   **the bone marrow of late-stage prostate cancer patients and**

254   **are correlated with worse progression free survival**

255   Liquid biopsies from peripheral blood and bone marrow

256   aspirate were acquired from a late-stage prostate cancer cohort

257   (NCT01505868). Matched bone marrow and peripheral blood

258   samples from 31 patients were analyzed for CTCs. CTCs with

259   increased genomic content (CTC-IGC), identified as having a

260   nuclear diameter at least double the average of the CTC cell

261   population, were found in 9.7% of peripheral blood samples. CTC-

262   IGC were present in 80.6% of bone marrow samples from the

263   same patients (Fig. 1A-B, S1). Survival analysis with 44 bone

264   marrow samples (from the 31 patients with matched blood

265   samples and 13 patients without matched blood) showed that

266   presence of at least one CTC-IGC detected in the bone marrow

267   was associated with decreased progression-free survival (Fig. 1C,

268   Table S1). Previous treatment history was available for 33 of the

269   44 patients and primarily included anti-androgens and other

270   hormonal treatments (i.e., bicalutamide, nilutamide,

271   enzalutamide). The six patients who were previously treated with

272   docetaxel were all positive for CTCs-IGC in the bone marrow.

273        Clonal tumor lineage measured via copy number ratio

274    analysis was confirmed in both typical CTCs and CTCs-IGC. No

275    apparent differences in copy number ratios were identified

276    between the two CTC groups (Fig. 1D-F, S2, S3). These

277    observations show that CTC-IGC can be found in blood and bone

278    marrow aspirate, are tumor derived, and thus may contribute

279    towards relapse in late-stage prostate cancer. Despite the

280    apparent WGD of CTC-IGC, these cells retain the original tumor

281    copy number profile. To understand the importance and behavior

282    of this phenotype, we used an *in vitro* model of polyploid tumor

283    cells to investigate their relationship with therapeutic resistance.

284

285    **Large polyploid cancer cells form as a response to**

286    **chemotherapy in prostate and breast cancer models**

287        PC3 and MDA-MB-231 cells were treated with sublethal

288    doses of docetaxel or cisplatin for 72 hours. Following

289    chemotherapy, cells were allowed to recover for 1 or 10 days in

290    their regular growth medium, lifted from culture, plated on

291    specialized glass slides, stained with cell and nuclear markers,

292    then imaged through high content scanning and evaluated for

293    nuclear size and other morphometric comparisons (Fig. 2A). While

294    there was significant cell death as expected (Fig. S4A), surviving

295    cells increased in both nuclear diameter and cell size as a function

296    of time (Fig. 2B-E; Fig. S4B).

297        To evaluate resistance, we treated cells that survived

298    cisplatin treatment (10 days post treatment; 10 DPT) with cisplatin

299    or docetaxel. Compared to the control condition (initially cisplatin

300    treated and then re-treated with DMSO) cell counts and cell

301    viability were not significantly impacted, suggesting that these

302    cells are not sensitive to additional rounds of chemotherapy (Fig.

303    S4A, S4D, 2E).

304        To obtain progeny cells from a single chemotherapy-

305    induced surviving polyploid cell, we isolated and single-cell

306    seeded PC3 cells 10 days post-cisplatin release (n=480) and 10

307    days post-docetaxel release (n=960) and monitored for colony

308    formation. From these, only 2 polyploid docetaxel-treated PC3

309    cells gave rise to progeny after 2 months (progeny-1) and 2.5

310    months (progeny-2). Progeny-2 failed to proliferate following the

311    first passage. Over the course of the three-month experiment,

312    approximately 50% of the polyploid cells treated with either

313    cisplatin or docetaxel remained viable and adherent.  The dividing

314    progeny-1 cells displayed a larger nuclear and cellular diameter

315    than the parental PC3 population from which it originated (Fig. 2F,

316    S4). We treated progeny-1 with docetaxel or cisplatin and found

317    that the population was sensitive to both chemotherapies. Further,

318    following 10 days of recovery, surviving progeny-1 cells had

319    increased nuclear and cell diameter, similar to what was observed

320    from the original parent population (Fig. 2F, S4B).

321    **Surviving PC3 polyploid cancer cells show no additional copy**

322    **number ratio alterations compared to parental controls**

323        To evaluate the presence of genomic alterations in the

324    surviving polyploid cells and their progeny, we assayed copy

12

325  number status and cell ploidy. Strikingly, surviving large polyploid

326  PC3 and MDA-MB-231 cells from both docetaxel and cisplatin

327  treatments showed no apparent copy number ratio differences

328  compared to control cells (Fig. 3A-C, S5). This result confirms

329  patient data in that copy number ratio status does not differ

330  between CTCs with normal nuclei and CTCs with larger nuclei

331  (Fig. 1D-F) and suggests that cells are undergoing complete WGD

332  rather than displaying specific copy number breakpoints. While

333  copy number status did display minor differences in the progeny-1

334  compared to parental control (e.g., an increased 3p gain) (Fig. 3A-

335  B), no substantial alterations were observed. Conversely, progeny-

336  2, the clone that did not survive the first passage, displayed the

337  most aberrant copy number profile compared to the other

338  conditions (i.e., 6 gain and 4p gain) and clustered separately from

339  the other PC3 cell conditions (Fig. 3A).

340        FISH probes for the centromeres of PC3 chromosome 1

341  (ploidy = 3) and chromosome 10 (ploidy = 1) showed no

342  statistically significant differences when comparing DMSO

343  parental control cells to progeny-1 cells (Fig. 3D), suggesting that

344  any apparent scars of ploidy reduction were not present. These

345  results prompted investigation into the phenotype of these

346  surviving cells.

347  **Single cell transcriptomic profiling reveals common genes**

348  **and pathways upregulated in PC3 and MDA-MB-231 polyploid**

349  **cells**

13

350    497 PC3 cells were isolated and sequenced in 5 separate

351    batches (Fig. S6) and included: DMSO control (n=129), 1-day

352    post-cisplatin release (n=78), 10 days post-cisplatin release

353    (n=68), 1-day post-docetaxel release (n=45), 10 days post-

354    docetaxel release (n=118), docetaxel progeny-1 (n=12), docetaxel

355    progeny-2 (n=13). Two batches of 203 MDA-MB-231 cells

356    included: DMSO control (n=43), 1-day post-cisplatin release

357    (n=22), 10 days post-cisplatin release (n=62), 1-day post-

358    docetaxel release (n=24), 10 days post-docetaxel release (n=62)

359    (Fig. S7).

360    Regardless of treatment, a general spatial separation that

361    was dependent on recovery duration was observed in PC3 and

362    MDA-MB-231 cells (Fig. 4A, S8). To identify convergent

363    phenotypes regardless of tumor type or therapy, we evaluated

364    genes that were upregulated in both PC3 and MDA-MB-231

365    following either cisplatin or docetaxel treatment. MDA-MB-231

366    cells 10 days post cisplatin or docetaxel release upregulated 1591

367    shared genes compared to DMSO control; PC3 cells 10 days post

368    cisplatin or docetaxel treatment upregulated 1178 shared genes

369    compared to DMSO control (LFC > 1.5, FDR < 0.01; Fig. 4B).

370    Intersection of the shared gene sets showed MDA-MB-231 and

371    PC3 cells that survive either cisplatin or docetaxel exposure

372    shared 309 upregulated genes (Fig. 4B; Table S2). The 309

373    shared genes were considered a survivor cell enrichment data set,

374    which was further evaluated.

14

375        Of the 309 shared genes, 77% were protein coding and

376    17% were lncRNAs, while the remaining ~6% were pseudogenes

377    or yet to be experimentally confirmed (TEC, not yet tested; Fig.

378    4C). Log-fold change values were plotted for PC3-Doc-DPT10 vs

379    MDA-Doc-DPT10 (Fig. 4D) and PC3-Cis-DPT10 vs MDA-Cis-

380    DPT10 (Fig. 4E). Within each treatment class, shared differentially

381    expressed genes (DEGs) were positively correlated between

382    MDA-MB-231 and PC3 cells, indicating the DEGs are upregulated

383    to a similar magnitude.

384        Common transcription factors (TFs) and hallmark

385    pathways upregulated in the survivors were delineated (Fig. 4F-

386    G). Two significantly enriched TFs, ZNF697 and NPAS2, were

387    previously reported in cells that transition out of senescence and

388    into a proliferative state [47]. Top enriched hallmark pathways in

389    the 309 gene survivor data set were: epithelial-to-mesenchymal

390    transition (EMT), upregulation of KRAS signaling, coagulation,

391    TNFa signaling via NFkB, and hypoxia (Fig. 4F). Single cell gene

392    enrichment confirmed the top upregulated hallmark pathways in

393    the shared survivor data set (Fig. 4H, S8-9). Additional pathways

394    identified to be significantly upregulated in the surviving cells

395    were: PI3K-AKT-mTOR Signaling, Inflammatory Response, and

396    Cholesterol Homeostasis (Fig. 4H, S8-9).

397

398    **Identification of HOMER1, TNFRSF9, and LRP1 as putative**

399    **chemotherapy RNA survival markers**

15

400        Utilizing the shared cell survivor gene set data, markers

401    were independently evaluated to understand their putative role in

402    chemotherapy survival and polyploid state. All 309 genes were

403    investigated via literature review and queried for terms in

404    September 2023, including: large tumor cell, polyploid giant

405    cancer cell, poly-aneuploid cancer cell, survival pathways, drug

406    resistance, chemotherapy, and apoptosis. With prior knowledge

407    that top upregulated genes (MMP-3, SAA1, and C3) functioned in

408    the execution of apoptosis and clearance of apoptotic bodies (Fig.

409    4D-E), and that SAA1 and C3 were correlated with better PFS

410    (Fig. S10), they were not considered novel survival markers. The

411    309 gene survivor cell enrichment data set was also intersected

412    with genes in the top enriched pathways that modulate survival:

413    TNFa via NFkB, PI3K-AKT, and mTOR signaling (Fig. 4G-H). We

414    identified TNFRSF9 and LRP1 as survival biomarkers; these are

415    known to function as cell surface receptors that enhance PI3K

416    activity. This activity, in turn, stimulates AKT, thereby promoting

417    cell survival (Fig. 4D-E, Fig. 5, S11A) [48-50]. Further, we

418    identified HOMER1 as a PC3-specific survival marker (Fig. 5);

419    HOMER1 plays a role in mTOR signaling and protection against

420    apoptosis [51-54].

421

422    **HOMER1, TNFRSF9, and LRP1 are protein markers of**

423    **chemotherapy survival and are retained in docetaxel treated**

424    **PC3 progeny**

425        At the protein level, we found surviving PC3 and MDA-MB-

426    231 cells post-chemotherapy treatment stained positive for

427    HOMER1, TNFRSF9, and LRP1 (Fig. 5A, 5D). Image

428    quantification revealed all PC3 conditions (except for progeny-1

429    cisplatin day 10 post-treatment release) were significantly

430    upregulated compared to controls (Fig 5A, 5C). Day 10 survivors

431    showed the highest protein expression levels for each marker

432    tested. Importantly, untreated PC3 progeny-1 displayed

433    significantly higher expression in all three survival markers tested

434    compared to parental DMSO control cells, suggesting these

435    markers were retained following treatment (Fig. 5A, 5C). CD45 is

436    typically utilized as a tumor cell exclusion marker that stains for

437    white blood cells. At day 10 post-treatment release time points we

438    noted a gain in CD45 protein expression that was retained in

439    progeny cells in PC3 cells (Fig. 5A, S10). MDA-MB-231 cells also

440    showed a significant upregulation of expression for most markers

441    tested, except HOMER1 for docetaxel day 10 post-treatment

442    release and LRP1 for cisplatin day 10 post-treatment release (Fig.

443    5D, 5F).

444

445    **HOMER1, TNFRSF9, and LRP1 are found at the protein level**

446    **patient BM samples, and their increased expression is**

447    **correlated with recurrence in public datasets**

448        A subset of bone marrow samples that displayed a high

449    frequency of CTC-IGC from the prostate cancer patient cohort

450    (Fig. 1) were stained with HOMER1, TNFRSF9, and LRP1 (Fig.

17

451    6A). Patient 1 and patient 3 did not participate in the clinical trial

452    but also displayed a high frequency of CTC-IGC (Table 1; see

453    methods). All patients profiled had CTCs that were positive for the

454    tested markers (Fig. 6B). While there were CTC-IGC positive for

455    the marker genes in each patient sample (Fig. 6A), the tested

456    markers were not selective for CTC-IGC (Fig. S12). Patient-5, who

457    displayed the highest percentage of CTCs positive for markers

458    HOMER1 and TNFRSF9, had the shortest PFS at 1.4 months

459    (Fig. 6B, Table 1). Additionally, these survival markers identified

460    cells in the bone marrow that displayed increased genomic

461    content but were negative for canonical epithelial markers (Fig.

462    S13).

463    In publicly available data for previously treated patients,

464    high expression of TNFRSF9 and LRP1 significantly correlated

465    with a shorter progression free survival in patients with prostate

466    cancer; HOMER1 was not statistically significant (p-value = 0.183)

467    (Fig. 6C). High gene expression of TNFRSF9, HOMER1, and

468    LRP1 were all significantly correlated with worse relapse free

469    survival in breast cancer (Fig. 6D). Taken together, we can

470    conclude the survival genes are associated with recurrence at the

471    RNA level and are present on CTCs-IGC in the bone marrow

472    aspirate of late-stage prostate cancer patients.

473    **4. Discussion**

474    Our analysis of bone marrow liquid biopsy samples from

475    previously treated advanced prostate cancer patients reveals that

18

476    the presence of polyploid cancer cells correlates with poorer

477    progression-free survival. Although clinical reports have frequently

478    observed polyploid cancer cells in later disease stages, a direct

479    link with disease recurrence has not been firmly established. We

480    also found that CTC-IGC have copy number profiles identical to

481    typical CTCs and are predominantly present in the bone marrow

482    rather than in peripheral blood.

483        Through single cell copy number profiling and the isolation

484    of progeny from individual polyploid cells, we demonstrate that the

485    polyploid cancer cell phenomenon represents a change in cell

486    state.

487        Single-cell copy number profiling shows that the copy

488    number ratios in patient CTC-IGC as well as chemotherapy

489    induced polyploid MDA-MB-231 and PC3 cells that survive

490    treatment are identical to those in their paired non-polyploid

491    samples. This indicates that these cells, either identified as patient

492    CTCs or those that survive in the days following therapy release *in*

493    *vitro*, undergo multiple rounds of WGD without any additional copy

494    number alterations. These findings provide crucial insights into the

495    dynamics and genetic stability of the polyploid cancer cell state.

496        Obtaining proliferative progeny proved challenging; after

497    three months of culturing single isolated polyploid cells, we

498    successfully derived only one proliferative progeny clone

499    (1/1,440). This outcome is significant for two main reasons: first, it

500    demonstrates that polyploid cancer cells can give rise to progeny,

501    but second, the extremely low success rate underscores why

19

502     these cells have historically been understudied. To enhance our

503     understanding, future research should employ high-throughput

504     techniques to isolate larger numbers of single cells, such as tens

505     of thousands, which may prove critical in understanding the roles

506     of non-proliferative polyploid cancer cells and assessing their

507     capabilities at reinitiating cell division to give rise to progeny.

508     Additionally, slight variations in the copy number profiles, such as

509     a 3p gain observed in the progeny-1 clone, hint at genomic

510     evolution. Further studies should explore this genomic evolution in

511     different progeny clones once they are sufficiently collected to

512     understand the dynamics of genomic re-organization in these

513     cells.

514         Through *in vitro* single cell transcriptomics, we further

515     provide evidence that polyploid cancer cells display a convergent

516     phenotype between MDA-MB-231 (breast cancer) and PC3

517     (prostate cancer) model systems. Despite being induced with

518     chemotherapies with contrasting mechanisms of action (cisplatin

519     and docetaxel), the different tumor models displayed a shared

520     polyploid signature of upregulating 309 common genes. This

521     convergence reveals significant insights into the biological

522     features of polyploid cancer cells.

523         In our observations, approximately 50% of polyploid cancer

524     cells remained attached to the culture flask in a non-proliferative

525     state during single cell progeny outgrowth experiments. Polyploid

526     cancer cells have been identified to progress through the cell

527     cycle but do not proliferate (i.e., endocycling or cytokinesis failure

20

528     occur before mitosis) [55]. This is hypothesized to be a protective

529     state of the cells that affords protection from therapeutic stressors.

530     This phenomenon aligns with our identification of ZNF697 and

531     NPAS2 as two transcription factors significantly enriched in the

532     convergent polyploid gene set that were previously identified to be

533     upregulated in cells that were in a non-proliferative state and

534     began re-initiating cell division [47]. This suggests that some

535     polyploid cells profiled on day 10 post therapy release may be

536     attempting to re-initiate proliferation since the chemotherapy has

537     been removed. This finding is further supported by a higher

538     percentage of cells at 10-DPT expressing more markers at the M-

539     phase of the cell cycle (Fig. S8-9). Future research should explore

540     the roles of ZNF697 and NPAS2 in polyploid cancer cells and their

541     implications for disease recurrence in progeny cells.

542        The convergent surviving cell gene set we identified

543     indicated that pro-survival and anti-apoptotic pathways, such as

544     TNFa via NFkB, PI3K-AKT, and mTOR signaling, are upregulated

545     in polyploid cancer cells [57-59]. Among the genes identified in

546     these pathways, TNFRSF9, HOMER1, and LRP1 were identified

547     as putative survival genes and were found to be upregulated at

548     the RNA and protein levels [48-54, 60-64]. Notably, these protein

549     markers were retained in the PC3 progeny-1 clone, suggesting

550     their upregulation in cells that survive chemotherapy. Additionally,

551     a subset of CTCs, including both polyploid and typical CTCs,

552     tested positive for TNFRSF9, HOMER1, and LRP1 at the protein

553     level. Of note, Patient 5, who experienced the shortest

21

554 progression-free survival at 1.4 months, had the highest

555 percentage of CTCs positive for the TNFRSF9 marker, indicating

556 that this gene may play a significant role in cancer cell survival.

557 Further, these markers identified a subset of cells with IGC that

558 were negative in the epithelial channel. These cells may be CTCs

559 that lost epithelial expression (i.e., EMT) and, in combination with

560 the upregulation of the proposed survival markers, could be adept

561 at surviving in the bone marrow. Further studies are needed to

562 evaluate the roles of TNFRSF9, HOMER1, and LRP1 in

563 chemotherapy resistance and as a biomarker to evaluate the

564 emergence of therapeutic resistance.

565        Our investigation of polyploid cancer cells confirms the

566 significant upregulation of hypoxia and cholesterol homeostasis

567 pathways. Studies have shown that targeting these pathways in

568 cell line models, including PC3 and MDA-MB-231, reduces the

569 viability of progeny from polyploid cancer cells [23,26]. Further

570 evidence comes from a study indicating that polyploid cancer cells

571 accumulate lipid droplets in response to chemotherapy [56],

572 underscoring the critical role of lipid balance as cells significantly

573 increase in size. These findings suggest that these pathways are

574 integral to the polyploid cancer cell state and represent promising

575 targets for therapeutic intervention.

576        The *in vitro* environment of cell culture does not always

577 recapitulate the *in vivo* nature of cancer cell biology. This makes it

578 difficult to speculate how polyploid cancer cells interact with their

579 neighboring malignant cells and the surrounding stroma.

22

580    Translating the findings of TNFRSF9, HOMER1, and LRP1 as

581    resistance markers in an *in vivo* model is a critical next step.

582    Future studies should employ mouse models or patient derived

583    xenografts and stain for these biomarkers to understand their

584    prominence *in vivo*. Further studies should also isolate polyploid

585    cancer cells through nuclear density to further understand their

586    cellular phenotypes in tumor tissue.

587            While patient results are promising, they also have

588    limitations. This study focuses on late-stage patients with

589    disseminated CTCs in the bone marrow and blood. The evaluated

590    cohort comprised advanced-stage patients whose previous

591    treatment regimens had failed. To minimize biases associated with

592    late-stage disease and to better understand initial treatment

593    responses and their role in inducing polyploid cancer cells, future

594    cohorts should include patients undergoing their first rounds of

595    therapy. One concern is that CTCs in peripheral blood are typically

596    found in later disease stages, potentially biasing our patient

597    population towards later stages. Obtaining samples from tissue,

598    blood, and bone marrow could address these concerns and

599    provide valuable insights into the role of polyploid cancer cells in

600    dissemination, initial response to therapy, and disease evolution.

601

## Declarations

602

23

605  participating in this study, without whom this research would not

606  have been possible. We thank the clinical and research consent

607  teams MDAnderson and the VA clinics for supporting the

608  enrollment of patients and sample collections.  Components of

609  figure 2 was created using Biorender.com.

620  **Ethics Approval and Consent to Participate**: The study was

621  conducted according to the guidelines of the Declaration of

622  Helsinki and approved by the Institutional Review Board of the

623  University of Southern California Keck School of Medicine, MD

624  Anderson (NCT01505868), and the VA of Los Angeles (PCC

625  2015-090980). Informed consent was obtained from all subjects

626  involved in the study.

627  **Data Availability**: Cell line scDNA-seq (GSE270567) and scRNA-

628  seq (GSE270568) are available through GEO. Patient scDNA-seq

629  is available upon reasonable request. Image data is available

630  upon reasonable request for cell lines and patients.

24

631    **Materials Availability**: If interested in using the High Definition

632    Single Cell Assay please contact CSI-Cancer.

633    **Code Availability**: Image analysis code is freely available at

634    https://github.com/aminnaghdloo/slide-image-utils. Downstream

635    analysis scripts (DNA-seq, RNA-seq, image quantification) are

636    available upon request.

637    **Author Contribution**: Conceptualization: M.J.S., R.K.P., K.J.P.,

638    S.R.A., and J.H.; Methodology: M.J.S., A.N., R.K.P.; Software:

639    M.J.S., A.N.; Formal analysis: M.J.S.; Investigation: M.J.S. and

640    M.K.; Resources: P.K. and J.H.; Writing - Original Draft: M.J.S.,

641    J.H, and  S.R.A.; Writing - Review & Editing: M.J.S., S.R.A.,

642    R.K.P., M.L., M.K., A.N., K.J.P, P.K., A.A, A.Z-W, P.C.;

643    Visualization: M.J.S.; Supervision: K.J.P., S.R.A., J.H.; Project

644    Administration: K.J.P., S.R.A., J.H.; Funding Acquisition: P.K.,

645    K.J.P., S.R.A., J.H., M.L.; Patient Accrual: M.L, R.C, I.P.G., A.A,

646    A.Z-W, P.C.

647    **Consent for Publication**: All the authors agree to publish this

648    paper.

649

## References

1. Kurbegovic, S., Berg, K.D., Thomsen, F.B., Gruschy, L., Iversen, P., Brasso, K., al.: The risk of biochemical recurrence for intermediate-risk prostate cancer after radical prostatectomy. Scand J Urol **51**, 450-6 (2017)

2. Goss, P.E., Ingle, J.N., Pritchard, K.I., Robert, N.J., Muss, H., Gralow, J., al.: Extending aromatase-inhibitor adjuvant therapy to 10 years. N Engl J Med **375**, 209-19 (2016)

3. Colleoni, M., Sun, Z., Price, K.N., Karlsson, P., Forbes, J.F., Thurlimann, B. al.: Annual hazard rates of recurrence for breast cancer during 24 years of followup: Results from the international breast cancer study group trials i to v. J Clin Oncol **34**, 927-35 (2016)

4. Bukowski, K., Kciuk, M., Kontek, R.: Mechanisms of multidrug resistance in cancer chemotherapy. Int J Mol Sci **21** (2020)

5. Ashdown, M.L., Robinson, A.P., Yatomi-Clarke, S.L., Ashdown, M.L., Allison, A., Abbott, D., al.: Chemotherapy for late-stage cancer patients: Meta-analysis of complete response rates. F1000Res **4**, 232 (2015)

6. Wang, X., Zhang, H., Chen, X.: Drug resistance and combating drug resistance in cancer. Cancer Drug Resist **2**, 141-60 (2019)

7. Cree, I.A., Charlton, P.: Molecular chess? hallmarks of anti-cancer drug resistance. BMC Cancer **17**, 10 (2017)

8. Siegel, R.L., Miller, K.D., Wagle, N.S., Jemal, A.: Cancer statistics, 2023. CA Cancer J Clin **73**, 17-48 (2023)

9. Trabzonlu, L., Pienta, K.J., Trock, B.J., De Marzo, A.M., Amend, S.R.: Presence of cells in the polyaneuploid cancer cell (pacc) state predicts the risk of recurrence in prostate cancer. Prostate **83**, 277-85 (2023)

10. Fei, F., Zhang, D., Yang, Z., Wang, S., Wang, X., Wu, Z., al.: The number of polyploid giant cancer cells and epithelial-mesenchymal transition-related proteins are associated with invasion and metastasis in human breast cancer. J Exp Clin Cancer Res **34**, 158 (2015)

11. Amend, S.R., Torga, G., Lin, K.-C., Kostecka, L.G., Marzo, A., Austin, R.H., al.: Polyploid giant cancer cells: Unrecognized actuators of tumorigenesis, metastasis, and resistance. Prostate 79, 1489-97 (2019)

12. Lopez-Sanchez, L.M., Jimenez, C., Valverde, A., Hernandez, V., Penarando, J., Martinez, A., al.: Cocl2, a mimic of hypoxia, induces formation of polyploid giant cells with stem characteristics in colon cancer. PLoS One **9**, 99143 (2014)

13. Was, H., Borkowska, A., Olszewska, A., Klemba, A., Marciniak, M., Synowiec, A., al.: Polyploidy formation in

cancer cells: How a trojan horse is born. Semin Cancer Biol **81**, 24-36 (2022)

14. Saleh, T., Carpenter, V.J., Bloukh, S., Gewirtz, D.A.: Targeting tumor cell senescence and polyploidy as potential therapeutic strategies. Semin Cancer Biol **81**, 37-47 (2022)

15. Ogden, A., Rida, P.C.G., Knudsen, B.S., Kucuk, O., Aneja, R.: Docetaxel-induced polyploidization may underlie chemoresistance and disease relapse. Cancer Lett **367**, 89-92 (2015)

16. Puig, P.-E., Guilly, M.-N., Bouchot, A., Droin, N., Cathelin, D., Bouyer, F., al.: Tumor cells can escape dna-damaging cisplatin through dna endoreduplication and reversible polyploidy. Cell Biol Int **32**, 103-{43 (2008)

17. Adibi, R., Moein, S., Gheisari, Y.: Zoledronic acid targets chemo-resistant polyploid giant cancer cells. Sci Rep **13**, 419 (2023)

18. Bielski, C.M., Zehir, A., Penson, A.V., Donoghue, M.T.A., Chatila, W., Armenia, J., al.: Genome doubling shapes the evolution and prognosis of advanced cancers. Nat Genet **50**, 1189-95 (2018)

19. Lopez, S., Lim, E.L., Horswell, S., Haase, K., Huebner, A., Dietzen, M., al.: Interplay between whole-genome doubling and the accumulation of deleterious alterations in cancer evolution. Nat Genet **52**, 283-93 (2020)

20. Pienta, K.J., Hammarlund, E.U., Austin, R.H., Axelrod, R., Brown, J.S., Amend, S.R.: Cancer cells employ an evolutionarily conserved polyploidization program to resist therapy. Semin Cancer Biol **81**, 145-59 (2022)

21. Pienta, K.J., Hammarlund, E.U., Axelrod, R., Brown, J.S., Amend, S.R.: Polyaneuploid cancer cells promote evolvability, generating lethal cancer. Evol Appl **13**, 1626-34 (2020)

22. Zhou, X., Zhou, M., Zheng, M., Tian, S., Yang, X., Ning, Y., al.: Polyploid giant cancer cells and cancer progression. Front Cell Dev Biol **10**, 1017588 (2022)

23. White-Gilbertson, S., Lu, P., Esobi, I., Echesabal-Chen, J., Mulholland, P.J., Gooz, M., al.: Polyploid giant cancer cells are dependent on cholesterol for progeny formation through amitotic division. Sci Rep **12**, 8971 (2022)

24. Zhou, M., Ma, Y., Chiang, C.-C., Rock, E.C., Butler, S.C., Anne, R., al.: Single cell morphological and transcriptome analysis unveil inhibitors of polyploid giant breast cancer cells in vitro. Commun Biol **6**, 1301 (2023)

25. Zhang, X., Yao, J., Li, X., Niu, N., Liu, Y., Hajek, R.A., al.: Targeting polyploid giant cancer cells potentiates a therapeutic response and overcomes resistance to parp inhibitors in ovarian cancer. Sci Adv **9**, 7195 (2023)

26. Carroll, C., Manaprasertsak, A., Bo elli Castro, A., Bos, H., Spierings, D.C., Wardenaar, R., Bukkuri, A., Engstr□om, N., Baratchart, E., Yang, M., et al.: Drug resilient cancer

27

cell phenotype is acquired via polyploidization associated with early stress response coupled to hif2 transcriptional regulation. Cancer research communications **4**(3), 691-705 (2024)

27. Marrinucci, D., Bethel, K., Kolatkar, A., Luttgen, M.S., Malchiodi, M., Baehring, F., al.: Fluid biopsy in patients with metastatic prostate, pancreatic and breast cancers. Phys Biol **9**, 016003 (2012)

28. Chai, S., Matsumoto, N., Storgard, R., Peng, C.-C., Aparicio, A., Ormseth, B., al.: Platelet-coated circulating tumor cells are a predictive biomarker in patients with metastatic castrate-resistant prostate cancer. Mol Cancer Res **19**, 2036-45 (2021)

29. Malihi, P.D., Morikado, M., Welter, L., Liu, S.T., Miller, E.T., Cadaneanu, R.M., Knudsen, B.S., Lewis, M.S., Carlsson, A., Velasco, C.R., Kolatkar, A., Rodriguez-Lee, M., Garraway, I.P., Hicks, J., Kuhn, P.: Clonal diversity revealed by morphoproteomic and copy number pro les of single prostate cancer cells at diagnosis. Converg Sci Phys Oncol **4**(1), 015003 (2018) https://doi.org/10.1088/2057-1739/aaa00b 2018 Jan 16

30. Chai, S., Ruiz-Velasco, C., Naghdloo, A., Pore, M., Singh, M., Matsumoto, N., al.: Identification of epithelial and mesenchymal circulating tumor cells in clonal lineage of an aggressive prostate cancer case. NPJ Precis Oncol **6**, 41 (2022)

31. Itseez: Open Source Computer Vision Library. https://github.com/itseez/opencv (2015)

32. Walt, S., Schonberger, J.L., Nunez-Iglesias, J., Boulogne, F., Warner, J.D., Yager, N., Gouillart, E., Yu, T., contributors: scikit-image: image processing in python. PeerJ **2**, 453 (2014) https://doi.org/10.7717/peerj.453

33. Baslan, T., Kendall, J., Ward, B., Cox, H., Leotta, A., Rodgers, L., al.: Optimizing sparse sequencing of single cells for highly multiplex copy number profling. Genome Res 25, 714-24 (2015)

34. Schmidt, M.J., Prabakar, R.K., Pike, S., Yellapantula, V., Peng, C.-C., Kuhn, P., al.: Simultaneous copy number alteration and single-nucleotide variation analysis in matched aqueous humor and tumor samples in children with retinoblastoma. Int J Mol Sci **24** (2023)

35. Krueger, F., James, F., Ewels, P., Afyounian, E., Weinstein, M., Schuster-Boeckler, B., Hulselmans, G., sclamons: FelixKrueger/TrimGalore: v0.6.10 (0.6.10). Zenodo (2023)

36. Kim, D., Paggi, J.M., Park, C., Bennett, C., Salzberg, F.P.: Graph-based genome alignment and genotyping with hisat2 and hisat-genotype. Nature Biotechnology **37**, 907-915 (2019) https://doi.org/10.1038/s41587-019-0201-4

37. Institute, B.: Picard. https://broadinstitute.github.io/picard/

38. Anders, S., Pyl, P.T., Huber, W.: Htseq – a python framework to work with high throughput sequencing data. bioinformatics **31**(2), 166-169 (2015)

39. Amezquita, R.A., Lun, A.T.L., Becht, E., Carey, V.J., Carpp, L.N., Geistlinger, L., al.: Orchestrating single-cell analysis with bioconductor. Nat Methods 17, 137-45 (2020)

40. Soneson, C., Robinson, M.D.: Bias, robustness and scalability in single-cell differential expression analysis. Nat Methods **15**, 255-61 (2018)

41. Keenan, A.B., Torre, D., Lachmann, A., Leong, A.K., Wojciechowicz, M.L., Utti, V., al.: Chea3: transcription factor enrichment analysis by orthogonal omics integration. Nucleic Acids Res **47**, 212-24 (2019)

42. Liberzon, A., Birger, C., Thorvaldsd ottir, H., Ghandi, M., Mesirov, J.P., Tamayo, P.: The molecular signatures database (msigdb) hallmark gene set collection. Cell Syst **1**, 417-25 (2015)

43. Noureen, N., Ye, Z., Chen, Y., Wang, X., Zheng, S.: Signature-scoring methods developed for bulk samples are not adequate for cancer single-cell rna sequencing data. Elife **11** (2022)

44. Lin, A., Yang, H., Shi, Y., Cheng, Q., Liu, Z., Zhang, J., al.: Pancansurvplot: A large-scale pan-cancer survival analysis web application. bioRxiv (2022)

45. Jain, S., Lyons, C.A., Walker, S.M., McQuaid, S., Hynes, S.O., Mitchell, D.M., al.: Validation of a metastatic assay using biopsies to improve risk stratification in patients with prostate cancer treated with radical radiation therapy. Ann Oncol **29**, 215-22 (2018)

46. Weigman, V.J., Chao, H.-H., Shabalin, A.A., He, X., Parker, J.S., Nordgard, S.H., al.: Basal-like breast cancer dna copy number losses identify genes involved in genomic instability, response to therapy, and patient survival. Breast Cancer Res Treat **133**, 865-80 (2012)

47. Martinez-Zamudio, R.I., Stefa, A., Nabuco Leva Ferreira Freitas, J.A., Vasilopoulos, T., Simpson, M., Dor e, G., al.: Escape from oncogene-induced senescence is controlled by pou2f2 and memorized by chromatin scars. Cell Genom **3**, 100293 (2023)

48. So, T., Croft, M.: Regulation of pi-3-kinase and akt signaling in t lymphocytes and other cells by tnfr family molecules. Front Immunol **4**, 139 (2013)

49. Luo, L., Wall, A.A., Tong, S.J., Hung, Y., Xiao, Z., Tarique, A.A., al.: Tlr crosstalk activates lrp1 to recruit rab8a and pi3ky for suppression of inflammatory responses. Cell Rep **24**, 3033-44 (2018)

50. He, Z., Wang, G., Wu, J., Tang, Z., Luo, M.: The molecular mechanism of lrp1 in physiological vascular homeostasis and signal transduction pathways. Biomedicine & Pharmacotherapy **139**, 111667 (2021)

849  51. Fei, F., Li, J., Rao, W., Liu, W., Chen, X., Su, N., al.:
850      Upregulation of homer1a promoted retinal ganglion cell
851      survival after retinal ischemia and reperfusion via
852      interacting with erk pathway. Cell Mol Neurobiol **35**, 1039-
853      48 (2015)
854  52. Luo, P., Zhao, Y., Li, D., Chen, T., Li, S., Chao, X., al.:
855      Protective effect of homer 1a on tumor necrosis factor-
856      alpha with cycloheximide-induced apoptosis is mediated by
857      mitogen-activated protein kinase pathways. Apoptosis **17**,
858      975-88 (2012)
859  53. Lv, W., Zhang, Q., Li, Y., Liu, D., Wu, X., He, X., al.:
860      Homer1 ameliorates ischemic stroke by inhibiting
861      necroptosis-induced neuronal damage and
862      neuroinflammation. Inflamm Res **73**, 131-44 (2024)
863  54. Reshetnikov, V.V., Bondar, N.P.: The role of stress-induced
864      changes of homer1 expression in stress susceptibility.
865      Biochemistry **86**, 613-26 (2021)
866  55. Kim, C.-J., Gonye, A.L., Truskowski, K., Lee, C.-F., Cho, Y.-
867      K., Austin, R.H., al.: Nuclear morphology predicts cell
868      survival to cisplatin chemotherapy. Neoplasia **42**, 100906
869      (2023)
870  56. Kostecka, L.G., Pienta, K.J., Amend, S.R.: Lipid droplet
871      evolution gives insight into polyaneuploid cancer cell lipid
872      droplet functions. Med Oncol **38**, 133 (2021)
873  57. Bhaskar, P.T., Hay, N.: The two torcs and akt. Dev Cell 12,
874      487-502 (2007)
875  58. Sharma, S., Yao, H.-P., Zhou, Y.-Q., Zhou, J., Zhang, R.,
876      Wang, M.-H.: Prevention of bms-777607-induced
877      polyploidy/senescence by mtor inhibitor azd8055
878      sensitizes breast cancer cells to cytotoxic
879      chemotherapeutics. Mol Oncol **8**, 469-82 (2014)
880  59. You, B., Xia, T., Gu, M., Zhang, Z., Zhang, Q., Shen, J., al.:
881      Ampk-mtor-mediated activation of autophagy promotes
882      formation of dormant polyploid giant cancer cells. Cancer
883      Res **82**, 846-58 (2022)
884  60. Smith, S.F., Collins, S.E., Charest, P.G.: Ras, pi3k and
885      mtorc2 - three's a crowd? J Cell Sci **133** (2020)
886  61. Dan, H.C., Antonia, R.J., Baldwin, A.S.: Pi3k/akt promotes
887      feedforward mtorc2 activation through ikk-alpha.
888      Oncotarget **7**, 21064-75 (2016)
889  62. Gaur, U., Aggarwal, B.B.: Regulation of proliferation,
890      survival and apoptosis by members of the tnf superfamily.
891      Biochem Pharmacol **66**, 1403{8 (2003)
892  63. Gonias, S.L., Campana, W.M.: Ldl receptor-related protein-
893      1: a regulator of inflammation in atherosclerosis, cancer,
894      and injury to the nervous system. Am J Pathol **184**, 18-27
895      (2014)
896  64. Terrand, J., Bruban, V., Zhou, L., Gong, W., El Asmar, Z.,
897      May, P., al.: Lrp1 controls intracellular cholesterol storage
898      and fatty acid synthesis through modulation of wnt
899      signaling. J Biol Chem **284**, 381-8 (2009)

30

**Figure legends**
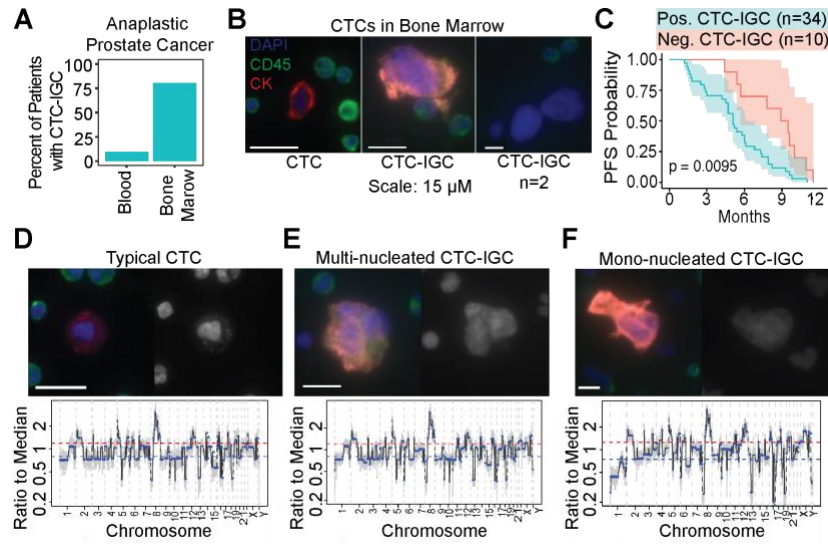


**Figure 1**: Large tumor cells are found in BM of late-stage prostate cancer patients. (A) Enumeration of patients with matched blood and bone marrow samples with at least 1 CTC-IGC present in liquid biopsy. (B) Representative images of CTC and CTC-IGC found in BM aspirate. Scale bars set to 15 µM. (C) PFS from patients with or without CTC-IGC found in BM samples. (D) Representative image of typical CTC found in BM with merged and DAPI channels (top) and its genomic copy number profile (bottom). (E) Representative image of CTC-IGC found in bone marrow with merged and DAPI images (top) and its genomic copy number profile (bottom). (F) Representative image of mono-nucleated CTC-IGC found in bone marrow with merged and DAPI images (top) and its genomic copy number profile (bottom).

31

917
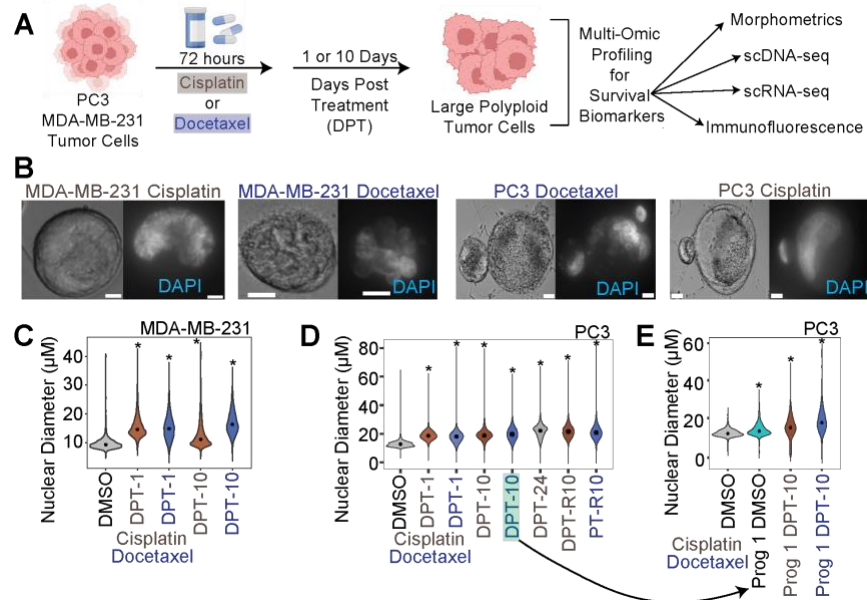
918 **Figure 2**: Large polyploid tumor cells are induced following
919 chemotherapy exposure in MDA-MB-231 and PC3 cell lineages.
920 (A) Experimental schematic for in vitro investigation of surviving
921 polyploid cells. (B) Representative bright field (left) and DAPI
922 (right) 40x images of MDA-MB-231 cells and PC3 cells treated
923 with docetaxel and cisplatin (right) 10 days post treatment
924 recovery. (C) Nuclear diameter for all treated conditions for MDA-
925 MB-231 cells. (D) Nuclear diameter for all treated conditions for
926 PC3 cells. Arrow indicates the condition where single cell progeny
927 originated from.  (E) Nuclear diameter of PC3 control parental and
928 progeny-1 cells, and progeny-1 10 days post-treatment cells.
929
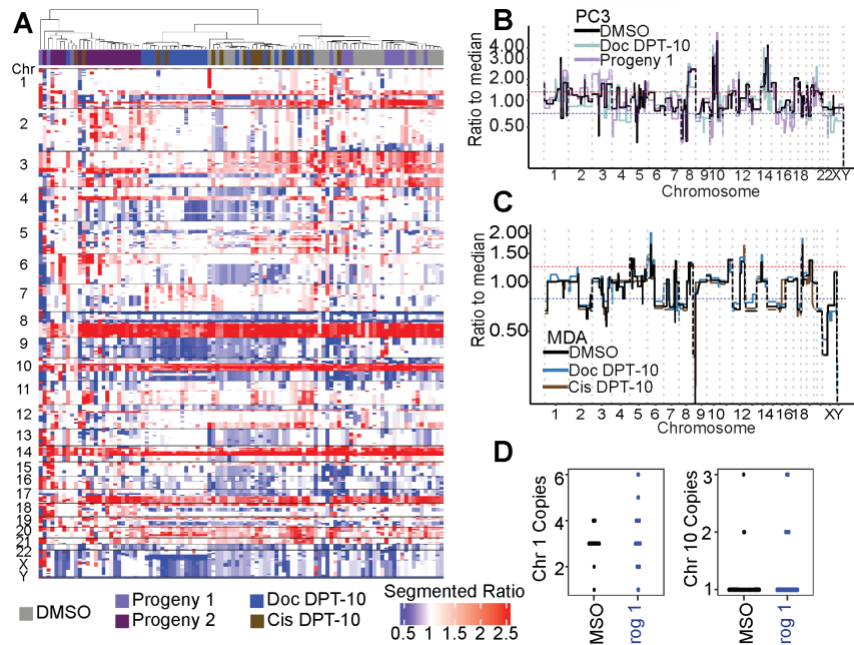
**Figure 3**: Genomics of PC3 DMSO control, docetaxel treated cells, and docetaxel large cell progeny-1. (A) Segmented copy number ratios for PC3 conditions. Ratio of 1 (white) indicates copy number neutral respective to the entire genome. (B) Representative PC3 DMSO, Doc D10, and Progeny-1 copy number ratio profiles. (C) Representative MDA-MB-231 DMSO control, Doc D10, and Cis D10 copy number ratio profiles. (D) FISH for PC3 DMSO control and progeny-1 cells for centromere of chromosome 1 (ploidy = 3) and chromosome 10 (ploidy = 1).
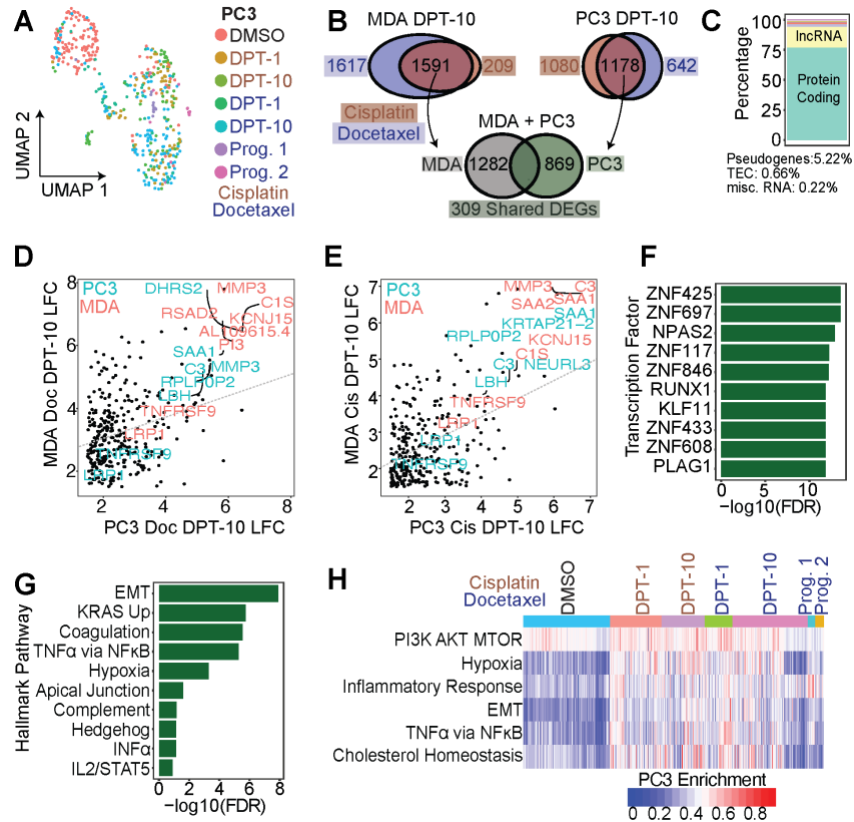
**Figure 4**: Chemotherapy induced surviving tumor cells share common phenotypes and pathways for survival. (A) UMAP of all conditions for PC3 cells. (B) Comparison of DEGs between MDA-MB-231 large-D10 and PC3 large-D10 cells. Between cisplatin and docetaxel treatments, MDA-MB-231 and PC3 share 309 upregulated genes compared to their respective controls. (B) Genecode annotations for 309 shared genes. (D-E) LFC of shared 309 genes for PC3 vs MDA-MB-231 for docetaxel and cisplatin treatments, respectively. (F) CHEA3 transcription factor enrichment of the shared 309 genes between MDA-MB-231 and PC3 cells. (G) Hallmark enrichment analysis of 309 shared genes. (H) Single cell Hallmark gene set enrichment analysis for all PC3 cells.
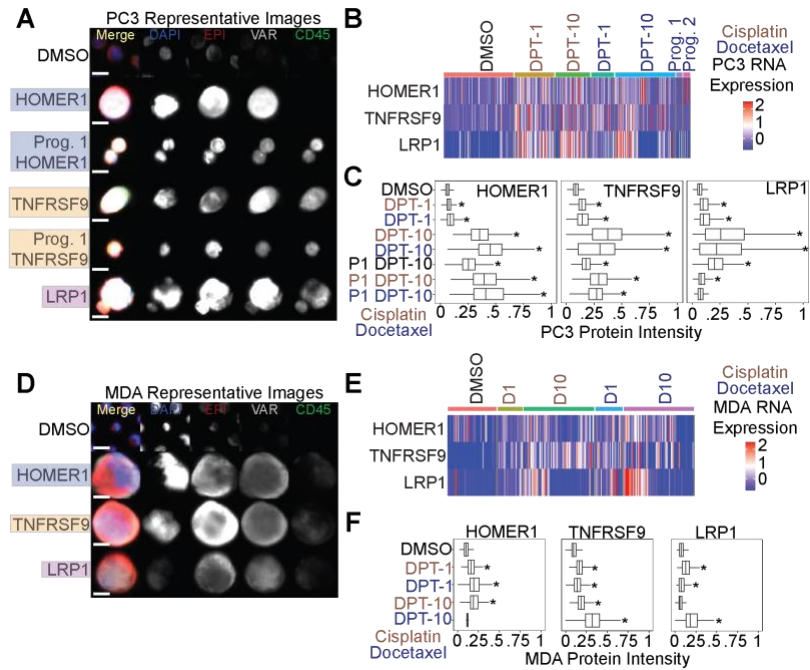
**Figure 5**: HOMER1, TNFRSF9, and LRP1 are putative markers of chemotherapy resistance. (A) Representative PC3 images of putative marker genes stain in the VAR (4th) channel. DMSO control cells were stained with HOMER1 and were negative. (B) RNA expression for each marker for all PC3 cells. (C) Immunofluorescence quantification for PC3 cells stained with tested markers. (D) Representative MDA-MB-231 images of putative marker genes stained in the VAR (4th) channel. DMSO control cells were stained with HOMER1 and were negative. (E) RNA expression for each marker for all MDA-MB-231 cells. (F) Immunofluorescence quantification for MDA-MB-231 cells stained with tested markers.
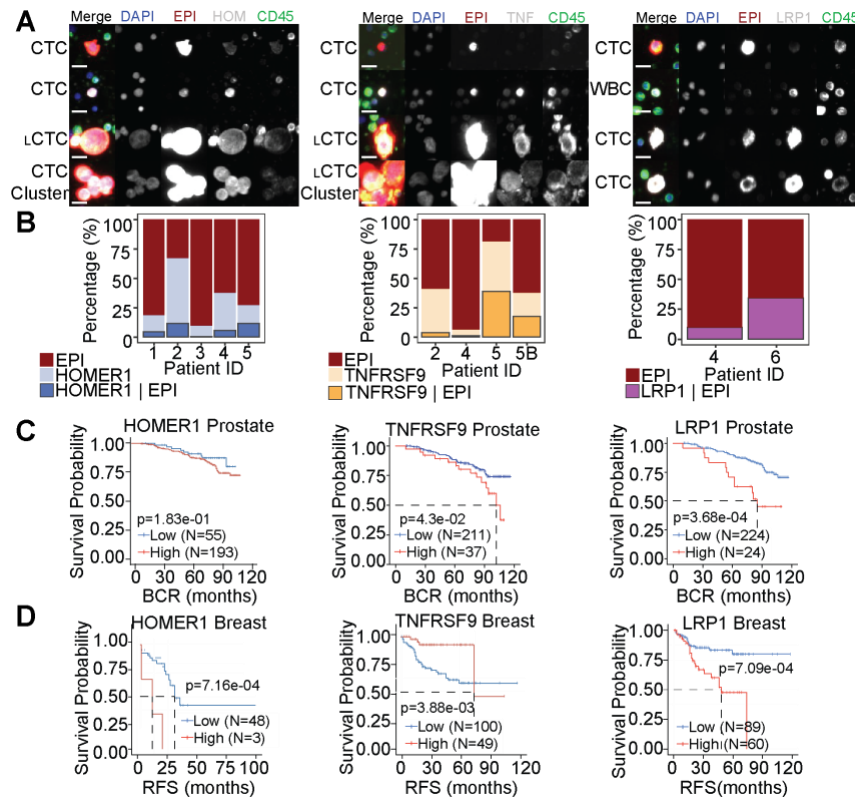
**Figure 6**: HOMER1, TNFRSF9, and LRP1 are positive on CTCs in the BM aspirate of late-stage prostate cancer and are correlated with recurrence in prostate and breast cancers. (A) Representative CTCs from BM of advanced prostate cancer patients that were stained with survival markers HOMER1 (left), TNFRSF9 (TNF; middle), and LRP1 (right). Tested markers appear as white in the merged image. Scale bars are 15 µM. (B) Percentages of CTCs with EPI positivity and cells that were stained with survival markers HOMER1 (left), TNFRSF9 (middle), and LRP1 (right). Cells that are positive for the marker alone (middle bar) cannot be conclusively labeled a tumor derived cell. LRP1 (right) is also a marker of T-cells, so only cells that were EPI positive were included. (C-D) Kaplan-Meyer survival plots for RNA expression of tested markers in prostate (C) and (D) breast cancer patients.